

Evolution of empty-state bands for Bi/GaAs(110): From Bi zigzag chains to ordered overlayers

Yongjun Hu, T. J. Wagener, M. B. Jost, and J. H. Weaver

Department of Chemical Engineering and Materials Science, University of Minnesota, Minneapolis, Minnesota 55455

(Received 20 January 1989)

We report studies of Bi-overlayer evolution on cleaved GaAs(110) using energy-dependent, momentum-resolved inverse photoemission (KRIPES) and low-energy electron diffraction (LEED). KRIPES results show a Bi-derived surface resonance at $E_F + 1.25$ eV on *n*-type GaAs(110) for 1–2 monolayer (ML) coverages of Bi. The same feature appears at $E_F + 1.45$ eV for *p*-type GaAs, and the 0.2-eV offset reflects the different Fermi-level pinning for *n*- and *p*-type GaAs(110). This Bi-induced feature exhibits no dispersion along $\bar{\Gamma}\bar{X}$ [001] but there is 0.2 eV upward dispersion along $[1\bar{1}0]$, consistent with Bi zigzag chain formation, bridging of Ga-As surface atoms along $[1\bar{1}0]$, and quasi-one-dimensional character with weak interaction between nearest-neighbor Bi chains. The surface is semiconducting for GaAs(110)-*p*(1×1) Bi (1 ML) with a gap of ~ 0.7 eV, and results for *n*- and *p*-type GaAs demonstrate independent development of band offset and barrier height. For Bi layers greater than 1 ML, a new LEED pattern, distorted along $[1\bar{1}1]$ or $[\bar{1}11]$, appears and persists to high coverage. For 2 ML, the surface is semimetallic, as reflected by a second Bi-derived empty state at $E_F + 0.35$ eV for *n*-type and $E_F + 0.55$ eV for *p*-type GaAs(110).

INTRODUCTION

There are very few overlayers on GaAs that are ordered and nondisruptive, but these few permit detailed investigation of the physics of evolving electronic states and Schottky barriers. Two such ordered overlayers are derived from Sb and Bi, elements which are semimetallic in bulk form. For Sb/GaAs, there is a rich experimental and theoretical literature.^{1–4} Although ordering of Bi overlayers on GaAs has only recently been discovered, several experimental studies have been reported. These include core-level photoemission investigations that demonstrated that the interface is disruption-free and angle-resolved photoemission that mapped the occupied energy bands.⁵

In this paper, we use momentum- or *k*-resolved inverse photoemission (KRIPES)^{6,7} to gain insight into the empty-electronic-state evolution for ordered Bi overlayers on GaAs(110). Of particular interest is the semimetallic or semiconducting character of the forming Bi overlayer, the correlation of empty states with interface structure, and the development of the Schottky barrier or heterojunction band offset. Our results show a Bi-derived state at 1.25 and 1.45 eV above E_F for *n*-type and *p*-type GaAs(110)-*p*(1×1) Bi (1 ML), respectively, with an energy difference that reflects different Fermi-level pinning positions. This state is enhanced for 1–2 monolayers (ML) of Bi but decreases with coverage. It shows no dispersion along the [001] direction, but there is 0.2 eV upward dispersion along $[1\bar{1}0]$. This behavior is related to the quasi-one dimensional zigzag chains of Bi atoms parallel to $[1\bar{1}0]$. For coverages greater than 1 ML, a second Bi-derived empty state develops just above E_F , consistent with semimetallic behavior, while a new ordered, Bi phase appears. For Bi coverages of ~ 5 ML, upward dispersion of 0.3 eV appears toward \bar{X}' .

EXPERIMENTAL TECHNIQUES

The experiments were performed in a spectrometer optimized for both ultraviolet and x-ray photon emission studies.⁸ This paper emphasizes KRIPES results in the photon-energy range of 10–44 eV. A highly collimated, monoenergetic electron beam was directed onto the sample surface from an electron gun with a 1×5 mm² planar BaO cathode and Pierce-type geometry. The emitted photons were dispersed by a near-normal-incidence grating monochromator and were detected with a position-sensitive detector. The combined energy resolution (electrons and photons) was 0.3–1 eV, depending on photon energy. The electron momentum resolution was better than 0.1 \AA^{-1} . The angle between the incident electron beam and outgoing photon beam was fixed at 60° while the angle of the incident electron beam relative to the sample surface normal ϕ , could be changed from 0° to 45° . Details of the spectrometer can be found elsewhere.⁸

GaAs(110) surfaces (*n*-type with Si doping at $4 \times 10^{18} \text{ cm}^{-3}$ and *p*-type with Zn doping at $3 \times 10^{18} \text{ cm}^{-3}$) were prepared by cleaving *in situ*. The deposition of Bi on the 300 K substrate was performed at pressures below 3×10^{-10} Torr; the base pressure of the experimental system was $\sim 8 \times 10^{-11}$ Torr. The amount of material deposited was determined with a quartz crystal oscillator. Surface structure for the evolving interface was investigated with LEED.

RESULTS AND DISCUSSION

In Fig. 1 we show representative KRIPES photon distribution curves (PDC's) for electrons incident normal to the surface, $k_{\parallel} = 0$, for Bi coverages $0 \leq \theta \leq 10$ ML on cleaved *n*-type GaAs(110). The amount of Bi deposited is given alongside each PDC with 3 \AA corresponding to ~ 1

ML of the ordered (1×1) overlayer, or 8.85×10^{14} atoms/cm². These spectra were taken with an incident electron energy $E_i = 16.25$ eV. They have been normalized to electron dose and the spectral throughput of the optical system to facilitate quantitative comparison. From Fig. 1 three main features are evident for clean *n*-type GaAs(110) at 1.3, 2.5, and 4 eV above E_F .⁹ Previous studies have shown that the 1.3 eV feature has a very large contribution from empty surface states while the other two structures represent bulk states.^{9,10} The deposition of 1 Å ($\sim \frac{1}{3}$ ML) of Bi shifts these GaAs(110)-derived peaks upward by 0.45 eV relative to E_F due to band-bending effects. At the same time, the intensity at the low-energy side of the surface-state feature is reduced as the surface becomes nearly unrelaxed.²⁻⁵ Unfortunately, Bi-derived features overlap with those of the substrate and make it difficult to accurately measure band-bending shifts above ~ 1 ML.

A very strong Bi-derived empty state, labeled *B* in Fig. 1, can be seen 1.25 eV above E_F for ~ 1 ML Bi on *n*-type GaAs(110). This state can first be seen at coverages of

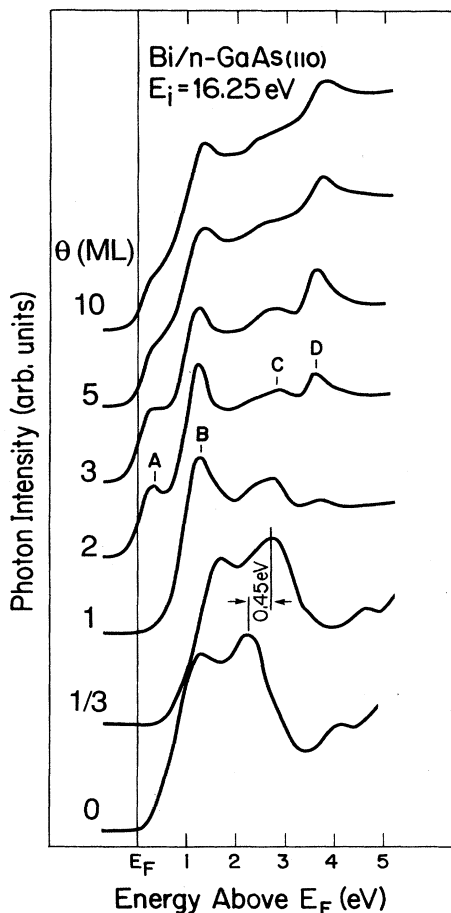


FIG. 1. Normal-incidence PDC's for 0–10 ML of Bi on cleaved *n*-type GaAs(110) taken with $E_i = 16.25$ eV. For 1 ML, there is a pronounced Bi-derived surface resonance, feature *B*, at 1.25 eV above E_F and the system is semiconducting. Feature *A* grows for 2 ML and reflects conversion to a semimetallic overlayer.

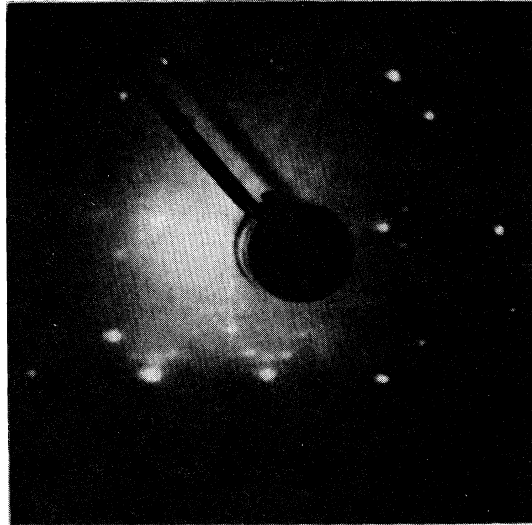
$\sim \frac{2}{3}$ ML. A similar Bi feature for *p*-type GaAs(110) appears at 1.45 eV at the same coverage. No Fermi edge can be seen at this coverage. Another Bi-derived state, labeled *A*, appears near E_F for coverages > 1 ML. It is 0.35 eV above E_F for *n*-type substrates for ~ 2 ML of Bi (0.55 eV E_F for *p*-type). With increasing deposition, it becomes less resolved from feature *B*, but it serves to pin the Fermi level. For higher coverages, other Bi-related states, labeled *C* and *D*, are seen at 2.7 and 3.7 eV above E_F .

The band evolution of Fig. 1, combined with the photoemission results of Ref. 5, indicates that 1 ML Bi/GaAs is semiconducting. Extrapolation of the leading edge of the PDC to zero intensity for 1 ML Bi/*p*-type GaAs places the conduction-band minimum (CBM) 0.7 eV above E_F . For the occupied states, there is a very low density of valence states to E_F , giving a band gap of 0.7 eV for 1 ML Bi on GaAs. This changes, however, with the growth of the second monolayer as peak *A* appears, and there is emission from states at E_F . The 2-ML case is then semimetallic and subsequent deposition shows no significant change in relation to the Fermi-level position at the Bi/GaAs(110) interface.

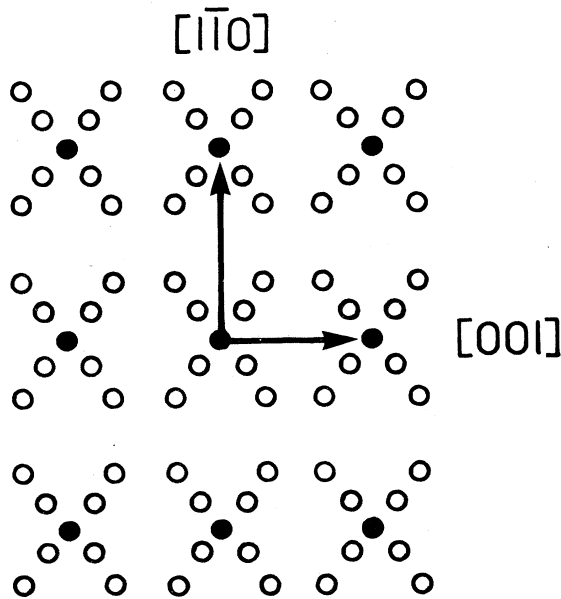
Parallel low-energy electron diffraction (LEED) investigations make it possible to correlate the changes in electronic states with overlayer structure. As expected, those results reveal indistinguishable growth morphologies for *n*-type and *p*-type GaAs(110) for starting surfaces of high quality. During the initial stage of Bi deposition at 300 K, namely ≤ 1 ML, a sharp $p(1 \times 1)$ pattern appears. In the sketch at the bottom of Fig. 2, the LEED spots for ordered GaAs(110)- $p(1 \times 1)$ Bi (1 ML) are identified by closed circles at the intersections of diagonals of open circles, corresponding to the $[1\bar{1}1]$ and $[\bar{1}11]$ directions, which represent the LEED spots that appear for > 1 ML. [The LEED pattern of Fig. 2 is for 5 ML Bi on GaAs(110).] The unit cell based on the LEED pattern for > 1 ML is not a simple two-dimensional Bragg lattice. Indeed, the Bi–As and Bi–Ga bond lengths differ for GaAs(110)- $p(1 \times 1)$ Bi (1 ML), an effect which is also reflected by distinguishable binding energies for Bi atoms coordinated to Ga and As (see Ref. 5). [Comparison to the Sb/GaAs case shows that the Sb–As bond length is slightly larger (~ 0.1 Å) than that of Sb–Ga (Refs. 2–4), and these differences are probably stronger for Bi/GaAs(110).] If we assume that Bi–Bi covalent bond lengths are unchanged, then the Bi layer will be distorted along $[1\bar{1}1]$ or $[\bar{1}11]$ for coverages > 1 ML. From the LEED pattern, one can see that the symmetry of the extra spots are all along the $[1\bar{1}1]$ and $[\bar{1}11]$ directions, consistent with the assumptions about bond lengths. It is likely that the distortion would give rise to the development of misfit dislocations. Indeed, the absence of the sixth LEED spot with periodicity in the $[1\bar{1}0]$ direction provides direct evidence for this misfit dislocation occurring every ~ 24 Å. Recent photoemission and Auger studies for Bi overlayer growth at 300 K have shown that the rate of attenuation of substrate emission exhibits a break at Bi coverages of 1 ML and that subsequent attenuation is characteristic of layer-by-layer growth.⁵ These results are in agreement with our LEED results be-

cause the latter show the persistence of ordered overlayer growth to coverages of at least 50 \AA ($\sim 16 \text{ ML}$) of Bi.

In Fig. 3 we present normal incident ($k_{\parallel}=0$) PDC's for incident electron energies from 13.25 to 19.25 eV for 2



(a)



(b)

FIG. 2. (a) LEED pattern of GaAs(110)+5 ML Bi at 300 K taken at 55 eV; (b) diagram of main diffraction spots representing a $p(1 \times 1)$ Bi (1 ML) overlayer (closed circles) and extra diffraction spots resulting from distortion along $[1\bar{1}1]$ or $[\bar{1}11]$ for coverages $> 1 \text{ ML}$ (open circles).

ML Bi on n -type GaAs(110). Features A , B , and D exhibit no dispersion with E_i , and thus with k_{\perp} , while the structure between 2 and 3 eV does disperse and is related to Bi bulk states or substrate features. Analogous development was observed for the empty electronic states for Bi on p -type GaAs(110) except that the energies were offset by 0.2 eV. This is related to the different positions of E_F in the gap for n - and p -type GaAs, as will be discussed.

Feature B is the first Bi-related structure to be observed (Fig. 1). It is not discernible for coverages less than $\sim \frac{1}{2} \text{ ML}$, is significant for $\sim \frac{2}{3} \text{ ML}$, and is prominent by 1 ML. This growth indicates that it depends strongly on the formation of Bi zigzag chains rather than Bi—GaAs bonding. Moreover, it is considerably stronger at lower incident electron energies ($E_i = 13.25\text{--}16.25 \text{ eV}$) than for higher energies (Fig. 3). This cross-section varia-

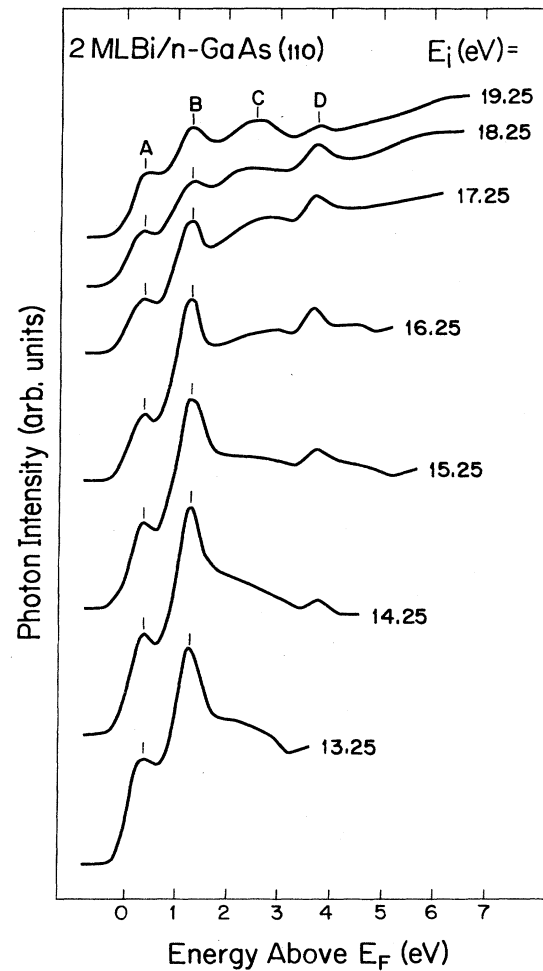


FIG. 3. Normal-incidence PDC's for 2 ML Bi on cleaved n -type GaAs(110) for incident electron energies $13.25 \leq E_i \leq 19.25 \text{ eV}$. The spectra show no dispersion of peaks A , B , and D with E_i and therefore k_{\perp} . Peak C disperses with k_{\perp} and is associated with a Bi bulk state or a substrate state.

tion indicates that it is predominantly p -like.^{11,12} Together these results suggest that feature B is derived from Bi-Bi p_z - p_z π^* chain bonds analogous to those predicted for Sb/GaAs by Mailhot *et al.*¹³ rather than Bi- p -GaAs sp^3 antibonding states, although the latter cannot be completely ruled out.

In Figs. 4 and 5, we present off-normal KRIPES spectra for $p(1 \times 1)$ Bi (1 ML) on p -type GaAs(110) for $E_i = 15.25$ eV. The resolution of the spectrometer for this energy is 0.3 eV. For the incident angles shown and the surface orientation, the spectra probe the surface Brillouin zone (SBZ) along $\bar{\Gamma}\bar{X}'$ and $\bar{\Gamma}\bar{X}$. For reference, the SBZ of GaAs(110) is presented at the bottom of Fig. 4. For 1 ML, there is again no emission close to E_F , there is no dispersion of feature B along $\bar{\Gamma}\bar{X}'[001]$, but there is a 0.2 eV upward dispersion toward \bar{X} , as summarized in Figs. 4 and 5. Analogous results for a 5 ML Bi overlayer show that feature B disperses upward by 0.3 eV for $\bar{\Gamma}\bar{X}'[001]$. (Feature B at $\bar{\Gamma}$ is shifted 0.15 eV toward E_F for the thicker film, as will be discussed below.) We conclude that feature B has weak dispersion along $[1\bar{1}0]$ for $p(1 \times 1)$ Bi (1 ML), corresponding to the zigzag chain direction of GaAs(110), but no dispersion perpendicular

to these chains. Together, these results indicate that feature B is quasi-one-dimensional, a conclusion reached for an empty Sb-derived state for GaAs(110)- $p(1 \times 1)$ Sb (1 ML).¹ For higher Bi coverages (e.g., ~ 5 ML), this quasi-one-dimensional character is changed as a new ordered structure appears.

In Fig. 6 we show KRIPES spectra at $E_i = 13.25$ eV with $\phi = 0^\circ, 5^\circ, 10^\circ,$ and 20° for an ordered 5 ML overlayer corresponding to this structure (ϕ is an angle between the incident electron beam and sample surface normal). Using the same labeling as above, features $A, B,$ and D appear at 0.75, 1.30, and 3.9 eV in normal incidence spectra. Comparison of the 1- and 5-ML results shows that features A and B at $\bar{\Gamma}$ are shifted 0.20 and -0.15 eV relative to E_F . The corresponding band structures along $\bar{\Gamma}\bar{X}'$ are presented in the inset of Fig. 6. Feature A now disperses 0.55 eV upward from $\bar{\Gamma}$ to near \bar{X}' while feature B , which did not disperse for 1 ML, shifts 0.3 eV. Features C and D shift 0.15 eV downward and 0.70 eV upward, respectively, along this direction.

We note that recent normal emission photoemission results have shown that a Bi-derived occupied state shifts from $E_F - 0.75$ eV at $h\nu = 15$ eV to $E_F - 1.05$ eV at $h\nu = 17$ eV for a 10 ML Bi overlayer on n -type GaAs(110). The Fermi level is located at the edge of this state. For coverages of 2 ML, no significant shifts for

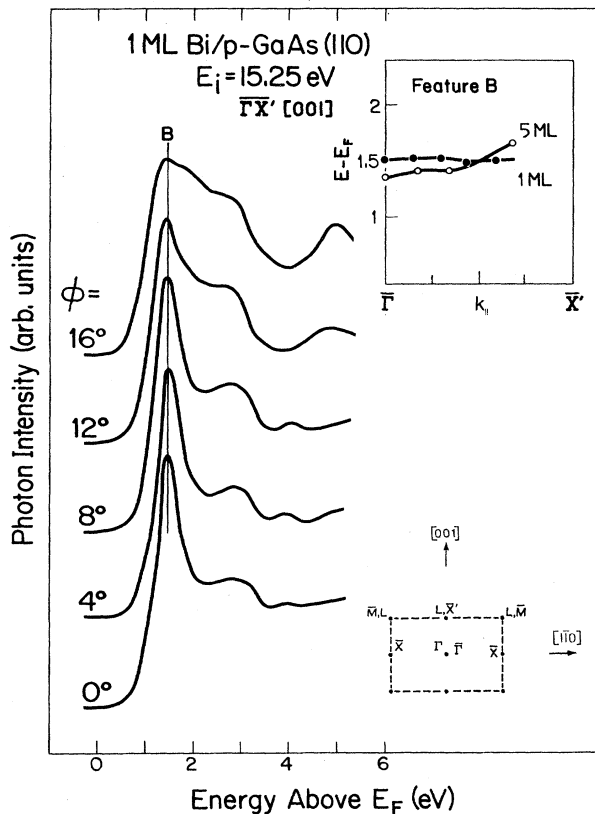


FIG. 4. PDC's for GaAs(110)- $p(1 \times 1)$ Bi (1 ML) for incident angles of $\phi = 0^\circ, 4^\circ, 8^\circ, 12^\circ,$ and 16° to investigate the empty states along $\bar{\Gamma}\bar{X}'[001]$ for $E_i = 15.25$ eV. As summarized in the inset, there is no dispersion of feature B (at 1.45 eV at $\bar{\Gamma}$ for p -type GaAs) for 1 ML of Bi but there is upward dispersion of ~ 0.30 eV toward \bar{X}' for 5 ML of Bi. The surface Brillouin zone is drawn at the lower right for reference.

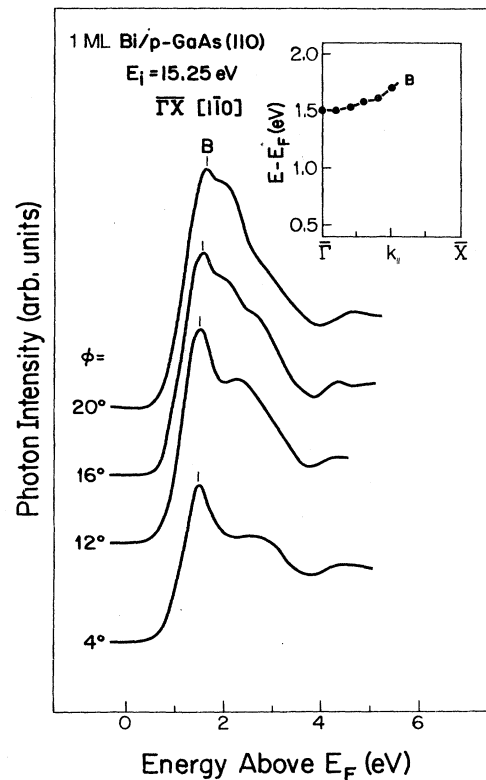


FIG. 5. PDC's for GaAs(110)- $p(1 \times 1)$ Bi (1 ML) analogous to those of Fig. 4 but with $\phi = 4^\circ, 12^\circ, 16^\circ,$ and 20° along $\bar{\Gamma}\bar{X}[1\bar{1}0]$ for $E_i = 15.25$ eV. The inset shows 0.2 eV upward dispersion of feature B . This dispersion represents the quasi-one-dimensional character of the Bi zigzag chains for 1 ML Bi.

this Bi-derived state can be found (less than 0.1 eV). Comparison with the KRIPES results indicates that the Bi-derived band structure at the Bi/GaAs(110) interface or for the low coverages of Bi (1–2 ML) remains quite two dimensional. For high coverages, the Bi-derived bands exhibit three-dimensional character.

To date, there have been no band calculations for Bi/GaAs, but calculations for GaAs(110)-*p*(1×1) Sb (1 ML) have been reported.^{2–4} Those treatments assumed that Sb adatoms formed zigzag chains with adatoms back bonding alternately to the Ga and As surface atoms of the nearly unrelaxed surface.^{10–12} This model has been confirmed by recent scanning tunneling microscopy images that showed Sb chains running along the $[1\bar{1}0]$ direction of GaAs (110) with each Sb atom covalently bonding to two adjacent Sb atoms.¹⁴ The calculations generally agree with each other, although the relative importance of Bi-GaAs *p-sp*³ and Bi-Bi π bonding differs.^{2–4} In light of the similarity of the Bi/GaAs and Sb/GsAs results, it seems reasonable to assume that Bi atoms are similarly backbonded. The nearest-neighbor Bi—Bi bonds and the

Bi—As backbonds are probably covalent while there is more ionic character for Bi—Ga backbonds.

For GaAs(110)-*p*(1×1) Bi (1 ML), we can suppose that parallel zigzag chains of Bi atoms form along the $[1\bar{1}0]$ direction. The relatively large separation between the Bi chains along $[001]$ results in very weak chain-to-chain interactions. [For GaAs(110)-*p*(1×1) Sb (1 ML), the Sb—Sb bond length in the chains is 2.8 Å in Ref. 3 and 2.87 Å in Ref. 4, while the distance between chains is ~ 5.65 Å.] The electronic structures projected along the direction perpendicular to the chains should then have no energy dispersion, consistent with our observation of very little or no dispersion along $\bar{\Gamma}\bar{X}'$ for feature *B* for 1 ML Bi. Likewise, the ~ 0.2 eV dispersion of feature *B* along $\bar{\Gamma}\bar{X}[1\bar{1}0]$ arises from the quasi-one-dimensional chains. The small dispersion of feature *B* also suggests that the Bi chains are strongly bonded to the GaAs(110) substrate.² This kind of bonding can dehybridize Bi states in the chain structure. It results in reduced bandwidth and reduced dispersion of empty *p* states along the chain direction (according to a simple calculation, an occupied 6*p* state bandwidth is ~ 1.5 eV for the Sb zigzag chain while a ~ 12 eV bandwidth of the 6*p* state is found for the linear chain²).

With coverages above 1 ML, a new ordered Bi structure forms on the top or hollow sites as suggested by the LEED results. These Bi overlayers deposited on the top of the chains provide a means for the interaction between nearest-neighbor chains. Experimentally, we see that feature *B* shows dispersion along $\bar{\Gamma}\bar{X}'$ at Bi coverages of 3–5 ML. The energy shift of feature *B* at $\bar{\Gamma}$ between 1 and 5 ML of Bi is probably related to Bi layer-layer interaction (Fig. 4). To our knowledge, this is the first observation of changes in energy dispersion from a quasi-one-dimensional to a two-dimensional unoccupied band structure as a result of interface morphology.

In Fig. 7 we show the intensity variation of feature *B*

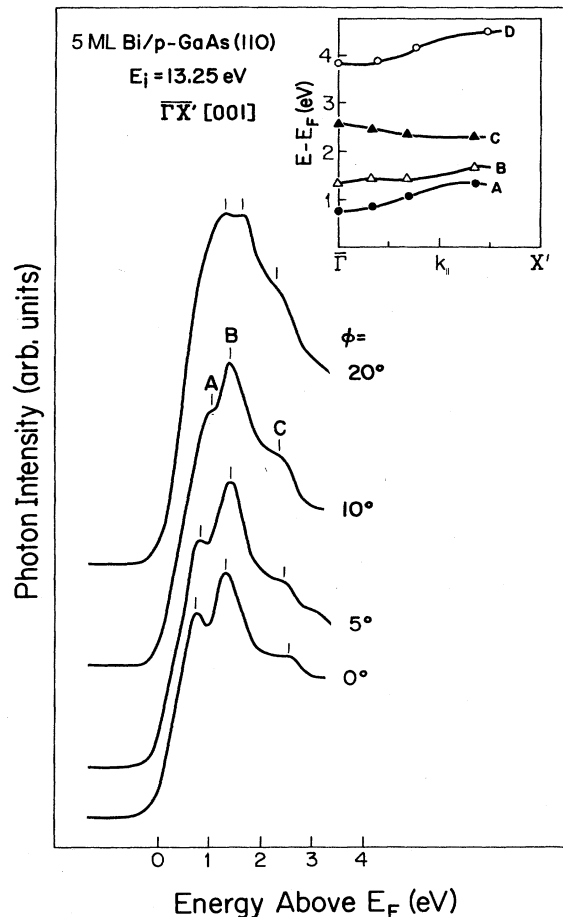


FIG. 6. PDC's for a 5 ML Bi on *p*-type GaAs(110) with $\phi = 0^\circ, 5^\circ, 10^\circ,$ and 20° along the $\bar{\Gamma}\bar{X}'[001]$ for $E_i = 13.25$ eV. The inset summarizes the empty bands projected along $\bar{\Gamma}\bar{X}'$ with upward dispersion of 0.30 and 0.55 eV for features *B* and *A*. Dispersion reflects the conversion to a two-dimensional overlayer by 5 ML Bi coverage.

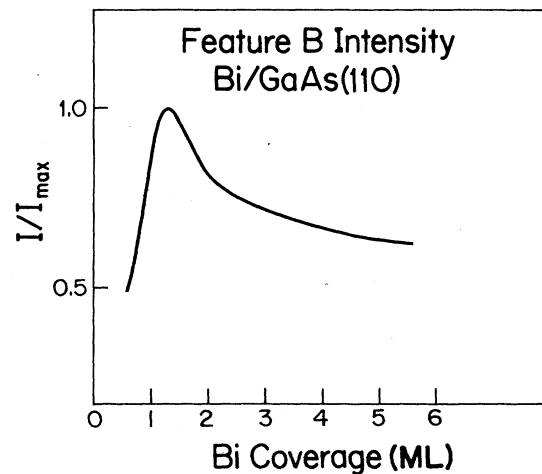


FIG. 7. Normalized intensity of feature *B* plotted as a function of Bi coverage showing the maximum in the surface resonance at 1.3 ML for $E_i = 15.25$ eV. This surface resonance couples to the bulk feature and eventually saturates to the bulk intensity at high coverage.

as a function of Bi coverage based on normal incidence data for $E_i = 15.25$ eV. As can be seen in Fig. 7, it reaches a maximum for coverages slightly greater than 1 ML, i.e., ~ 1.3 ML. This reveals that adding a small number of Bi adatoms ($\sim \frac{1}{3}$ ML) on hollow sites between chains enhances the interaction of the Bi chain states. Feature *B* is only enhanced for 1–2 ML coverages of Bi and then decreases because the resonating chain states are localized at the interface. Eventually, feature *B* saturates at 50% of its peak intensity since a bulk state couples with the interface state. The interaction between the first monolayer and further overlayers is also seen from the slight shift of feature *B* at $\bar{\Gamma}$.

We noted above that feature *A* only appears for coverages greater than 1 ML, indicating that it can be attributed to overlayer states rather than a surface resonance. Significantly, the Fermi level position is finally located at the edge of this state. As can be seen in Fig. 3, feature *A* shows an E_i dependence that is somewhat similar to that of a feature *B* and we propose that it also has predominantly *p*-like (*6p*) character. With increasing deposition from 1 to 6 ML, this state shifts ~ 0.2 eV, an effect we attribute to Bi layer-layer interactions.

Feature *D* appears after the *p*(1 \times 1) Bi (1 ML) structure is grown and it has typical two-dimensional character (Figs. 1, 3, and 6). The intensity of feature *D* is dependent on the surface or cleave quality. We suggest that it is related to an image potential state on the ordered Bi surface.¹³ For the best unpinned, mirrorlike surfaces, the intensity of this feature increases from 1 ML to higher coverages (e.g., ~ 3 ML) as can be seen in Fig. 1. This probably reflects the change from a semiconducting epi-

taxial layer to a semimetallic thin film (the image potential state is easier to see in the case of a metal than a semiconductor).

Finally, we noted above that the energy positions of the Bi-derived states varied by 0.2 eV for (1 \times 1) Bi (1 ML) overlayers on *n*- and *p*-type GaAs(110). This difference is very close to the ~ 250 meV offset observed for the pinning positions for Sb layers grown on *n*- and *p*-type GaAs.¹⁵ According to photoemission results for Bi/GaAs, the pinning positions differ by a value that is very close to 0.2 eV.⁵ It reveals that the positions of the Bi-derived features with respect of the VBM of GaAs(110) for an *n*-type substrate are the same as those for *p*-type. This indicates that Bi-derived features for GaAs(110)-*p*(1 \times 1) Bi (1 ML) are fixed relative to the VBM of GaAs(110), giving no dependence of the Fermi-level positions. These results can be understood from the fact that “band offset” or conduction-band-edge discontinuity at the interfaces of GaAs(110)-*p*(1 \times 1) Bi (1 ML) is independent of the Fermi-level positions. Recent photoemission studies have shown similar results that band offset (valence-band discontinuity) development and barrier-height formation occur independently at the Ge/GaAs(001) heterojunction interfaces.^{16,17}

ACKNOWLEDGMENTS

This work was supported by the National Science Foundation under Grant No. DMR-86-10837. Discussions with G. J. Lapeyre, J. J. Joyce, G. D. Waddill, and F. Xu are gratefully acknowledged.

¹W. Drube and F. J. Himpsel, Phys. Rev. B **37**, 855 (1988).

²P. Skeath, C. Y. Su, W. A. Harrison, I. Lindau, and W. E. Spicer, Phys. Rev. B **27**, 6246 (1983).

³C. M. Bertoni, C. Calandra, F. Mangli, and E. Molinari, Phys. Rev. B **27**, 1251 (1983).

⁴C. Mailhot, C. B. Duke, and D. J. Chadi, Phys. Rev. B **31**, 2213 (1985).

⁵J. J. Joyce, J. R. Anderson, M. M. Nelson, C. Yu, and G. J. Lapeyre (private communication).

⁶J. B. Pendry, Phys. Rev. Lett. **45**, 1356 (1980); J. Phys. C **14**, 1381 (1981).

⁷V. Dose, Prog. Surf. Sci. **13**, 225 (1983); F. J. Himpsel, Comments Condens. Mater. Phys. **12**, 199 (1986); N. V. Smith, Rep. Prog. Phys. **51**, 1227 (1988).

⁸Y. Gao, M. Grioni, B. Smandek, J. H. Weaver, and T. Tyrie, J. Phys. E **21**, 488 (1988).

⁹D. Straub, M. Skibowski, and F. J. Himpsel, Phys. Rev. B **32**, 5237 (1985).

¹⁰Y. Gao, T. J. Wagener, Yongjun Hu, and J. H. Weaver (unpublished).

¹¹Th. Fauster and F. J. Himpsel, Phys. Rev. B **30**, 1874 (1984).

¹²J. J. Yeh and I. Lindau, Data Nucl. Data Tables **32**, 51 (1985); **32**, 53 (1985); **32**, 103 (1985).

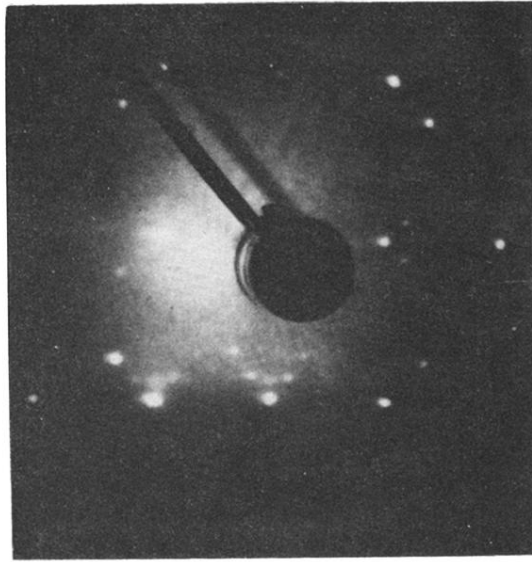
¹³M. Weinert, S. L. Hulbert, and P. D. Johnson, Phys. Rev. Lett. **55**, 2055 (1985).

¹⁴R. M. Feenstra and P. Mårtensson, Phys. Rev. Lett. **61**, 447 (1988).

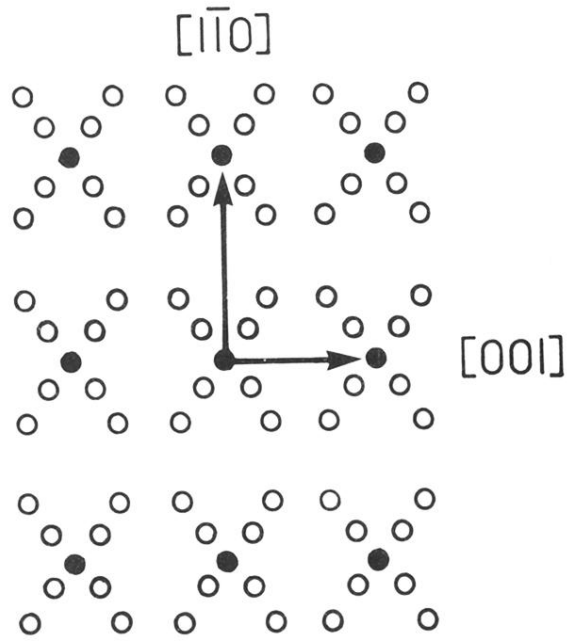
¹⁵R. Cao, K. Miyano, I. Lindau, and W. E. Spicer, Appl. Phys. Lett. **53**, 137 (1988).

¹⁶P. Chiaradia, A. D. Katnani, H. W. Sang, Jr., and R. S. Bauer, Phys. Rev. Lett. **52**, 1246 (1984).

¹⁷S. A. Chambers and T. J. Irwin, Phys. Rev. B **38**, 7484 (1988).



(a)



(b)

FIG. 2. (a) LEED pattern of GaAs(110)+5 ML Bi at 300 K taken at 55 eV; (b) diagram of main diffraction spots representing a $p(1 \times 1)$ Bi (1 ML) overlayer (closed circles) and extra diffraction spots resulting from distortion along $[1\bar{1}1]$ or $[\bar{1}11]$ for coverages > 1 ML (open circles).